The separation of mass, momentum and heat transfer scales in particle-laden detonations

Daniel Martínez-Ruiz[1], César Huete[2], Antonio L. Sánchez[3]

[1]Universidad Politécnica de Madrid, Madrid, Spain
[2]Universidad Carlos III de Madrid, Leganés, Madrid, Spain
[3]University of California San Diego, La Jolla, CA, USA

1 Introduction

Detonations of particle-laden flows are of wide interest to the scientific community: in hypersonic propulsion with liquid fuel droplets, dust explosions with solid reacting particles, or mitigation of risks with water sprays over reactive gaseous mixtures. The underlying physics involve complicated transfer processes of mass, momentum and energy between the carrier gas and the disperse phase (either liquid or solid), that requires a detailed modeling.

First approaches comprised the response of shock waves in dusty gas flows when drag effects are present in the two-phase coupling [1], but soon other effects, such as heat transfer, were incorporated to non-reactive flows [2]. The particles traversing the shock wave are typically considered to remain unaffected and preserve their speed and temperature prior to the shock. This approximation addresses the fact that a relaxation region must appear in which drag forces decelerate the particles to the compressed flow velocity and heat transfer rises their temperature to their thermal equilibrium with the carrier. In the case of liquid particles or droplets traversing a shock, breakup processes can be avoided for sufficiently small values of the Weber number [3], given very fine droplet sizes which will be considered here. Nevertheless, the exchange of mass between phases must then be considered to account for the vaporization processes [4, 5], which also alters the energy exchange. Finally, some other studies have incorporated the reactive nature of detonations either for particles [6] or droplets [7, 8].

However, a systematic study on the characteristic length scales that appear in the physical problem related to the accommodation, heating and vaporization times [9], and their competition with the typical induction length of detonations is yet to be offered. For this purpose, the present work considers a multi-continua formulation, given that mono-disperse particles can be distributed closely together, with inter-particle distances ℓ_d much smaller than the macroscopic length-scale of the problem L, but still much larger than the particle radius a [10]. This limit enables an Eulerian formulation of the disperse phase, which acts as an ideal continuous media when disregarding inter-particle interactions.

2 Formulation

We shall first consider a shock passage over particle-laden mixtures in a 1-D steady-state approximation. The disperse phase is formed by a dilute monodisperse distribution of fuel droplets, as sketched in Fig.1, such that its volume fraction is $\phi_d = (\frac{4\pi}{3}a^3)/(\ell_d^3 - \frac{4\pi}{3}a^3) \ll 1$, where subscript d is used hereafter for

Correspondence to: daniel.mruiz@upm.es

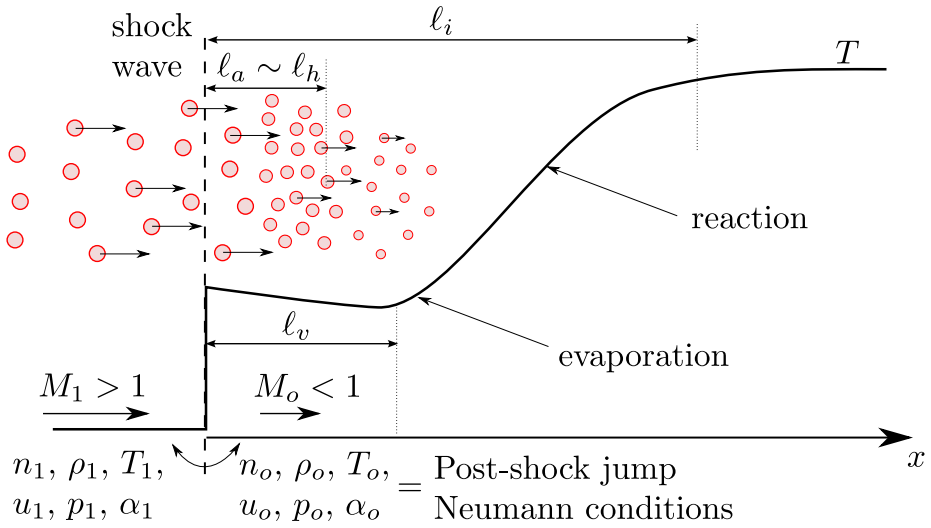

Figure 1: One-dimensional detonation internal structure for a monodisperse fuel spray. Physical scales involved in the accommodation (ℓ_a), heating (ℓ_h), evaporating (ℓ_v) and reactive (ℓ_i) processes.

droplet variables. The former allows to define the particle number density, $n = \ell_d^{-3}$. Therefore, as the disperse-phase (liquid or solid) density is much larger than the gaseous phase $\rho_d/\rho \sim \mathcal{O}(10^3)$, the liquid-to-gas mass-loading ratio can be defined as

$$\alpha = \frac{\frac{4\pi}{3}a^3\rho_d}{\ell_d^3\rho} = \frac{m_d n}{\rho}, \tag{1}$$

and takes values of order unity when $(a/\ell_d)^3 \sim \rho/\rho_d$. For this reason, a two-continua formulation for the gaseous and solid or liquid phases can be used for characteristic lengths $L \gg \ell_d \gg a$, where the macroscopic scale encloses numerous particles that are sufficiently separated from each other.

Regarding the two-way coupling between phases, drag-force modeling f_x must be provided first. Stokes flow may be used for a velocity difference between the gas and liquid phase $(u-u_d)$, if the particle-based Reynolds number is small $\mathrm{Re_d} \ll 1$, be $f_x = 6\pi\mu a(u-u_d)$. Nevertheless, for large Reynolds numbers $\mathrm{Re_d} \gg 1$ the drag expression $f_x = \rho C_D a^2(u-u_d)^2$ can be applied without qualitative changes in the character of the results. Each drag model involves an adaptation time $t_a \sim m_d u_0/f_x$. In particular, for Stokes flow ($Re_d \ll 1$) around the particles, $t_a = m_d/(6\pi\mu a) = (2\rho_d a^2)/(9\rho_0\nu_0)$, defines the accommodation length $\ell_a = u_o t_a$.

Additionally, a source term of mass vaporization rate $\dot{m}_d$ must be included to describe the varying radius of droplets a. Specifically, the Eulerian individual droplet mass change reads

$$\frac{d\left(\frac{4\pi}{3}\rho_d a^3\right)}{dt} = \frac{4\pi}{3}\rho_d u_d \frac{da^3}{dx} = -\dot{m}_d = -4\pi a \frac{k}{c_p}\lambda, \tag{2}$$

where

$$\lambda = \frac{1}{\mathrm{Le}_v}\log\left(\frac{1-Y_v}{1-Y_{v,s}}\right) \tag{3}$$

is the dimensionless vaporization rate for a local mass fraction of vapour Y_v and a particularized amount on the droplet surface $Y_{v,s}$, which is provided by the Clausius-Clapeyron relation, namely,

$$Y_{v,s} = \frac{W_v}{W_s}\exp\left(\frac{L_v}{RT_B} - \frac{L_v}{RT_d}\right), \tag{4}$$

with Le_v standing for the Lewis number of the vapour, T_B the boiling temperature, L_v the latent heat of vaporization, W_v the molecular mass of the vapor fuel and $W_s = (Y_{v,s}/W_v + Y_{O,s}/W_O)^{-1}$ the molecular mass of the mixture at the droplet surface. Hereafter, a new time scale must be introduced, controlled by the vaporization rate model, which scales as $t_v \sim a^2\rho_d/(3\rho D_T)$, such that $t_a/t_v = 2/(3Pr)$.

Finally, the heat transferred from the gas phase $\dot{q}_g = 4\pi ka(T - T_d)\mathrm{Nu} = L_v\dot{m}_d + \dot{q}_d$ includes the additional phase-change energy transfer and heating rate for each droplet, which is then expressed as

$$\dot{q}_d = 4\pi ka\left(\frac{T - T_d}{e^\lambda - 1} - \frac{L_v}{c_p}\right)\lambda, \tag{5}$$

with $\lambda/(e^\lambda - 1)$ corresponding to the Nusselt number of a evaporating sphere, Stefan flow considered, and k the conductivity of the mixture.

The gas phase conservation equations for steady one-dimensional flows along the x direction read,

$$\begin{aligned}
\frac{d}{dx}(\rho u) &= n\dot{m}_d, && (6)\\
\frac{d}{dx}(\rho u^2) &= -\frac{dp}{dx} + n\dot{m}_d u_d - nf_x, && (7)\\
\frac{d}{dx}(\rho u c_p T) &= u\frac{dp}{dx} - nf_x(u_d - u) + -n\left[\dot{m}_d(L_v - c_pT_d) + \dot{q}_d\right] + Q\dot{\omega}, && (8)\\
\frac{d}{dx}(\rho u Y_v) &= n\dot{m}_d - \dot{\omega}, && (9)\\
\frac{d}{dx}(\rho u Y_O) &= -s\dot{\omega} && (10)\\
p &= \rho RT, && (11)
\end{aligned}$$

for continuity, momentum, enthalpy, fuel vapor species Y_v, oxidizer species Y_O and equation of state respectively. Specifically, R is the universal gas constant, Q is the heat release per unit mass of fuel consumed and s the amount of oxidizer consumed per unit mass of fuel. The reaction rate $\dot{\omega}$ is described with a 1-step irreversible global Arrhenius model,

$$\dot{\omega} = B\rho Y_v Y_O \exp\left(-\frac{E_a}{RT}\right), \tag{12}$$

where B is the pre-exponential factor, and E_a the activation energy.

The disperse liquid-phase equations are

$$\begin{aligned}
\frac{4\pi}{3}\rho_d u_d\frac{da^3}{dx} &= -\dot{m}_d = -4\pi a\frac{k}{c_p}\lambda, && (13)\\
\frac{4\pi}{3}\rho_d a^3 u_d\frac{du_d}{dx} &= f_x = 6\pi\mu a(u - u_d), && (14)\\
\frac{4\pi}{3}\rho_d a^3 u_d c\frac{dT_d}{dx} &= \dot{q}_d = 4\pi ka\left(\frac{T - T_d}{e^\lambda - 1} - \frac{L_v}{c_p}\right)\lambda, && (15)\\
\frac{d}{dx}(nu_d) &= 0 && (16)
\end{aligned}$$

use made of the direct transformation of $d/dt = \partial/\partial t + u_d\partial/\partial x$ from a Lagrangian evolution into an Eulerian formulation.

The integration of the system of equations requires boundary conditions at $x = 0$ corresponding to post-shock properties (Neumann conditions noted with the subscript o), $\rho - \rho_o = u - u_o = T - T_o = n - n_o = u_p - u_1 = T_p - T_1 = 0$. Post-shock conditions can be expressed as functions of the incoming Mach number $M_1 = u_1/\sqrt{\gamma R T_1}$ (with specific heats ratio $\gamma = c_p/c_v$) through the well-known Rankine-Hugoniot relations for velocity $u_o/u_1 = \rho_1/\rho_o = f_u(M_1, \gamma)$, pressure $p_o/p_1 = f_p(M_1, \gamma)$, temperature $T_o/T_1 = f_T(M_1, \gamma)$, or the resulting Mach number $M_o = f_M(M_1, \gamma)$.

3 Scales of the reactive problem

On one hand, the main length scale of the reactive flow dynamics is given by the induction length ℓ_i, which will be used together with the post-shock gas speed u_o to write the characteristic reactive-flow time, $t_c = \ell_i/u_o$. On the other hand, the aforementioned droplet acceleration time, use made of the Stokes-flow approximation, is $t_a = 2\rho_d a^2/(9\rho\nu)$. Those two time scales introduce the dimensionless Stokes number $St = t_a/t_c$, describing the inertia of the droplets relative to the reactive gas flow.

Dimensionless coordinates are then $\eta = x/\ell_i$, and $\tau = t/(\ell_i/u_o)$. In addition, the dimensionless flow variables are referred to post-shock values, namely $\rho' = \rho/\rho_o$, $u' = u/u_o$, $T' = T/T_o$, $p' = p/(\rho_o u_o^2)$, $Y_O' = Y_O/Y_{Oo}$, $a' = a/a_o$, $n' = n/n_o$, $T_d' = T_d/T_o$, $u_d' = u_d/u_o$. Finally, some dimensionless parameters appear, as $q = Q/c_p T_o$, $S = s/Y_{Oo}$, $T_B' = T_B/T_o$ and $l_v = L_v/(c_p T_o)$.

The two-way coupled set of equations can now be written in dimensionless form, for the gas phase,

$$\frac{d}{d\eta}(\rho u) = \frac{2}{3}\frac{\alpha_o n a \lambda}{\mathrm{PrSt}}, \tag{17}$$

$$\frac{d}{d\eta}(\rho u^2 + p) = \frac{\alpha_o n a \lambda}{St}\left(\frac{2}{3}\frac{u_d \lambda}{\mathrm{Pr}} - (u - u_d)\right), \tag{18}$$

$$\frac{d}{d\eta}(\rho u T) = (\gamma - 1)M_o^2\left[u\frac{dp}{d\eta} + \frac{\alpha_o n a}{\mathrm{St}}(u - u_d)^2\right] - \frac{2}{3}\frac{\alpha_o n a \lambda}{\mathrm{PrSt}}\left(\frac{T - T_d}{e^\lambda - 1} - T_d\right) + q\dot{\Omega}, \tag{19}$$

$$\frac{d}{d\eta}(\rho u Y_v) = \frac{2}{3}\frac{\alpha_o n a \lambda}{\mathrm{PrSt}} - \dot{\Omega}, \tag{20}$$

$$\frac{d}{d\eta}(\rho u Y_O) = -S\dot{\Omega}, \tag{21}$$

$$p = \frac{\rho T}{\gamma M_o^2}, \tag{22}$$

where the tildes have been dropped for convenience, and with $\mathrm{Pr} = \nu/(k/\rho c_p) = 0.7$, the mass-loading ratio $\alpha_o = (4/3)\pi a_o^3 n_o(\rho_d/\rho_o)$ and the dimensionless reaction rate $\dot{\Omega} = \beta\rho Y_{Oo} Y_O Y_v \exp(\beta(1 - 1/T))$, where $\beta = E_a/RT_o$ is the Zeldovich number. It should be noted that the characteristic induction length selected above is, thus, $\ell_i = \beta^{-1}(u_o/B)e^\beta$. Secondly, for the liquid phase we have

$$u_d\frac{da^2}{d\eta} = -\frac{4}{9}\frac{\lambda}{\mathrm{PrSt}}, \tag{23}$$

$$a^2 u_d\frac{du_d}{d\eta} = \frac{u - u_d}{\mathrm{St}}, \tag{24}$$

$$a^2 u_d\frac{dT_d}{d\eta} = \frac{2}{3}\frac{c_p/c\lambda}{\mathrm{PrSt}}\left(\frac{T - T_d}{e^\lambda - 1} - l_v\right), \tag{25}$$

$$\frac{d}{d\eta}(n u_d) = 0. \tag{26}$$

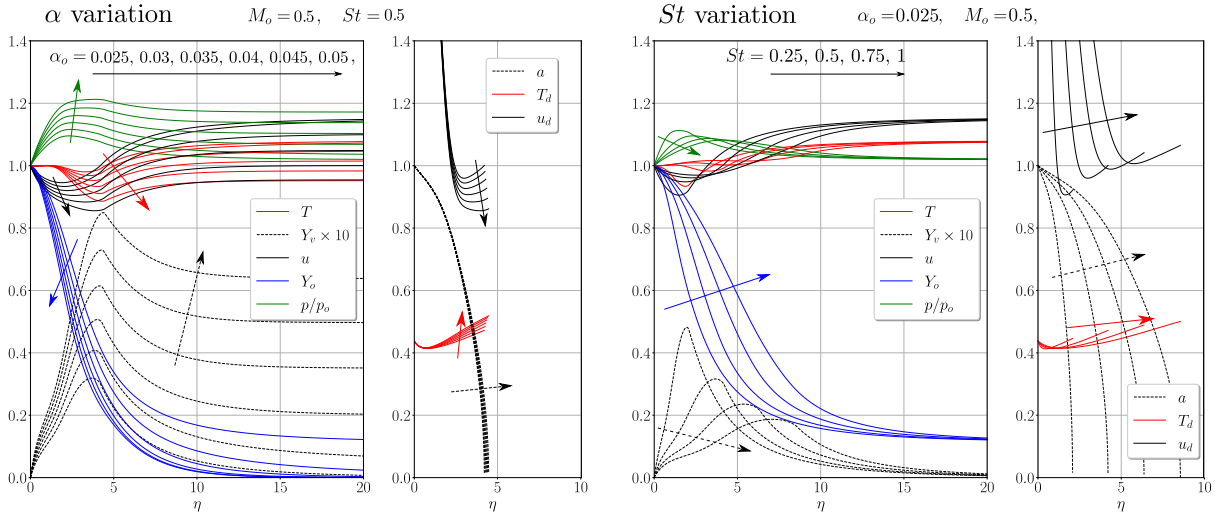

Figure 2: Numerical results for variation of the mass-loading ratio (left) and the Stokes number (right).

4 Results

Characteristic values provided here for discussion include the latent heat of vaporization of methanol $L_v \simeq 1100 kJ/kg$, which will be used in the following. Its boiling temperature ranges from $T_B = 337\,K$ at 1 bar to $T_B = 400\,K$ at 8 bar, the later being the pressure provided by normal shocks at $M_1 = 2.645$ or $M_o = 0.5$, and the specific heat ratio is taken as $c/c_p = 2.5$. Reactive parameters are fixed to $\beta = 10$, $q = 5$ and $S = 6$ for convenience. Representative results of the integration are shown in Fig. 2 for progressive variation of the mass-loading ratio parameter α_o and for variation of the inertia of the droplets via the Stokes number. It should be noted that the relaxation zone remains practically unaffected by the variation of the liquid mass in the disperse phase, while the final momentum and thermal equilibrium value is strongly controlled by this parameter. However, droplet inertia through variation of the Stokes number produces major changes in the competing lengths and the inner structure of the relaxation-induction region with practically constant downstream equilibrium values for fixed Mach number and mass-loading ratio. Different modifications of the competing lengths involved, be induction, accommodation, heating and vaporization, through Zeldovich, Stokes, Prandtl numbers and c/c_p, have shown in additional computations to provide different regimes of detonations, either overdriven, Chapman-Jouguet or failure.

Finally, the formulation presented above is used to obtain the upstream Mach number that suffices to provide sonic state ($M = 1$) in the post-shock flow, be the Chapman-Jouguet condition, for varying values of the parameters presented above. Figure 3 shows the upstream Mach number providing CJ detonation regime for fixed values of α_o and St, together with the distance from the shock where sonic conditions are achieved. It can be noted that increasing mass-loading ratio requires stronger shock waves to provide the CJ regime, while differences in droplet inertia are mostly irrelevant when varying the Stokes number. Finally, a maximum value of α_o is found, for which the distance of sonic conditions $x_{\rm CJ}$ grows asymptotically. As a concluding remark, large amounts of liquid droplets of a prescribed fuel can lead to failure due to the great thermal requirements of heating and vaporization processes that need to be balanced with combustion heat release.

Acknowledgements
Projects TED2021-129446B-C41 and TED2021-129446B-C43 funded by MCIN/AEI / 10.13039 / 501100011033 and European Union NextGenerationEU/ PRTR. D.M.R. and C.H. work has been also supported by the Madrid Government (Comunidad de Madrid-Spain) under the Multiannual Agreement

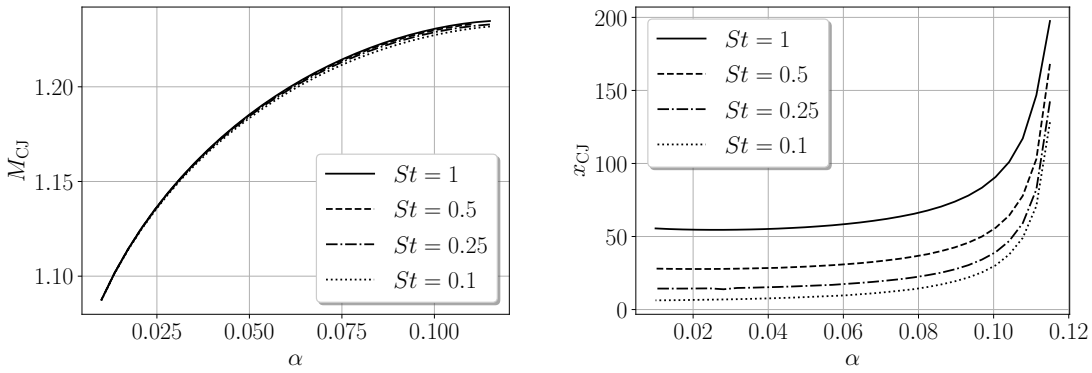

Figure 3: Variation of Chapman-Jouguet Mach number (left) and distance (right) for variation of α_o and different values of the droplets Stokes number.

with UPM (CHAC-CM-UPM) and UC3M (H2SFE-CM-UC3M).

References

[1] Carrier, G. F. (1958). Shock waves in a dusty gas. Journal of Fluid Mechanics, 4(4), 376-382.

[2] Rudinger, G. (1964). Some properties of shock relaxation in gas flows carrying small particles. The Physics of Fluids, 7(5), 658-663.

[3] Theofanous, T. G. (2011). Aerobreakup of Newtonian and viscoelastic liquids. Annual Review of Fluid Mechanics, 43, 661-690.

[4] Evans, P. J., & Mackie, J. C. (1971). Shock-Wave Interaction with an Evaporating Aerosol. The Physics of Fluids, 14(3), 539-541.

[5] Kersey, J., Loth, E., & Lankford, D. (2010). Effect of evaporating droplets on shock waves. AIAA journal, 48(9), 1975-1986.

[6] Fan, B. C., & Sichel, M. (1989). A comprehensive model for the structure of dust detonations. In Symposium (International) on Combustion (Vol. 22, No. 1, pp. 1741-1750).

[7] Kailasanath, K. (2006). Liquid-fueled detonations in tubes. Journal of Propulsion and Power, 22(6), 1261-1268.

[8] Lu, T., & Law, C. K. (2004). Heterogeneous effects in the propagation and quenching of spray detonations. Journal of propulsion and power, 20(5), 820-827.

[9] Sánchez, A. L., Urzay, J., & Liñán, A. (2015). The role of separation of scales in the description of spray combustion. Proceedings of the Combustion Institute, 35(2), 1549-1577.

[10] Martínez-Ruiz, D., Urzay, J., Sánchez, A. L., Liñán, A., & Williams, F. A. (2013). Dynamics of thermal ignition of spray flames in mixing layers. Journal of fluid mechanics, 734, 387-423.